Least-squares wavelet analysis and its applications in geodetic and geophysical time series analyses

Ebrahim Ghaderpour (1,2), E. Sinem Ince (1,3), and Spiros Pagiatakis (1)

1-Earth and Space Science and Engineering, Lassonde School of Engineering, York University, Canada
2- Department of Mathematics and Statistics, The University of Calgary, Canada
3-Helmholtz Centre Potsdam, German Research Centre for Geosciences (GFZ), Potsdam, Germany

EGU2018-11109-3

Summary

We propose a new method of analyzing a time series as well as a method to compute the coherency between two (or more) time series. These methods, namely, the **least-squares wavelet analysis (LSWA)** and the **least-squares cross wavelet analysis (LSCWA)**, respectively, can analyze any time series that exhibit non-stationarity, while they may be unequally spaced, and unequally weighted, exhibiting gaps and offsets **without the need of editing** them.

1) Least-squares wavelet analysis (LSWA)

Definition: Decomposition of a time series into time-frequency domain by an appropriate segmentation of the series and calculation of spectral peaks based on the least-squares fit of sinusoids to each segment.

- Segmentation is achieved by a translating window whose size is characterized by the number of data points included.
- The size of the window $L(\omega_k) = \left\lfloor \frac{L_1 M}{\omega_k} \right\rfloor + L_0$ must include a number of data points to achieve a reasonable redundancy for the least-squares fit where M: sampling interval, L_1: number of cycles of the base function, ω_k: frequency of the base function (dilation), L_0: additional number of data points considered to achieve the desired time and frequency resolution.

For a fixed frequency, the window length varies in translation while its size remains constant for unequally spaced time series (Fig. 1a), but the window length and size are both constant in translation for equally spaced time series (Figs. 1b and 2).

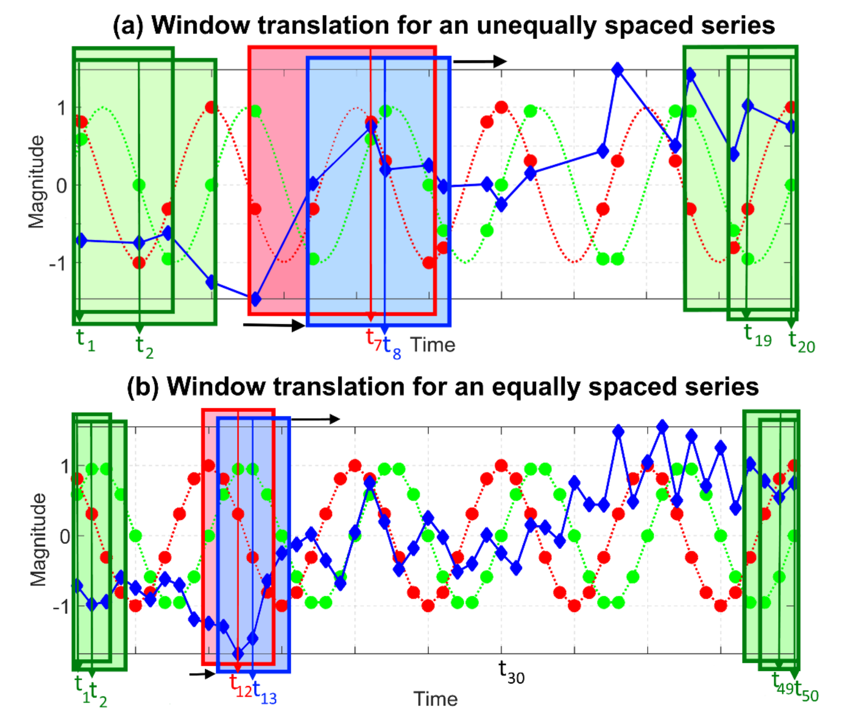

Fig. 1) **(a)** Unequally spaced and **(b)** Equally spaced time series along with sinusoids (*cosine - red and sine - green*) and some windows

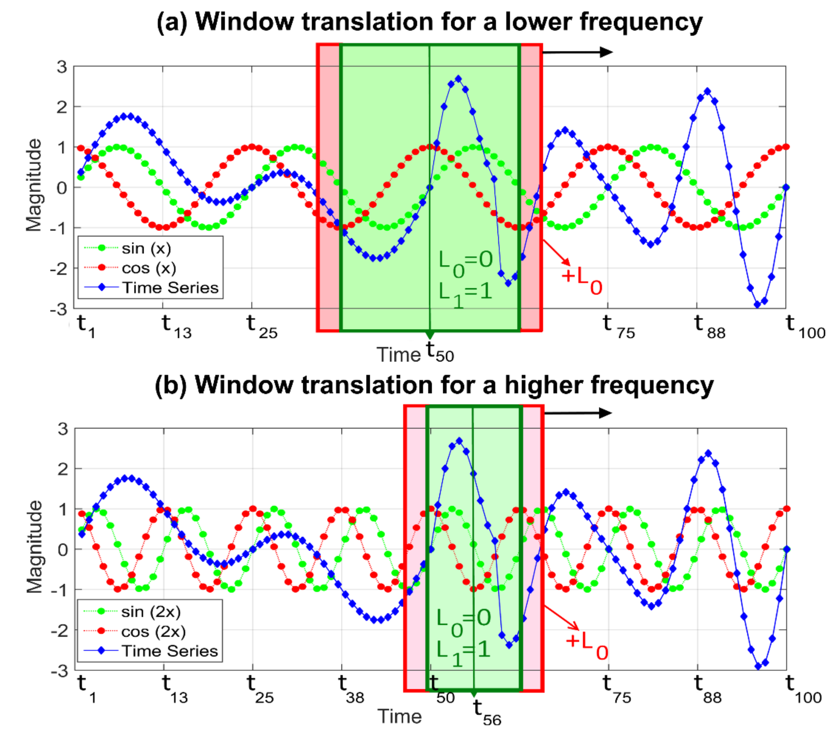

Fig. 2) Window translation of an equally spaced time series (*blue*) for **(a)** sin(x) and cos(x) and **(b)** sin(2x) and cos(2x).

2) Continuous wavelet transform (CWT) vs least-squares wavelet spectrogram (LSWS)

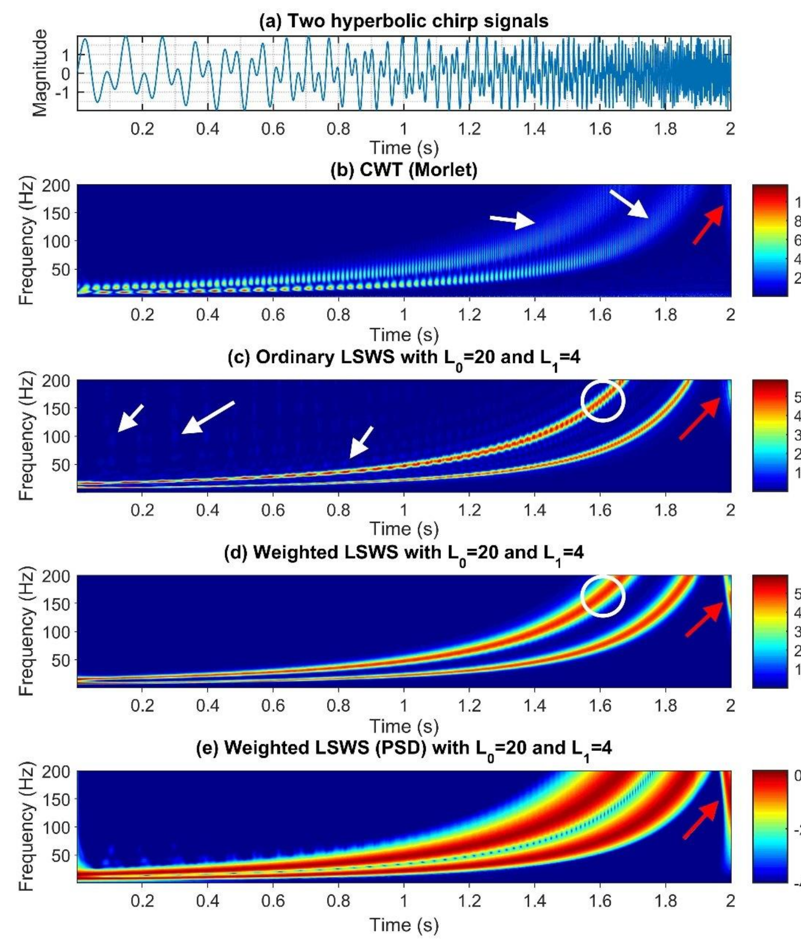

Fig. 3) Two hyperbolic chirp signals and their analyses.

$$f_1(t_i) = \cos\left(\frac{230}{2.3 - t_j}\right) + \cos\left(\frac{500}{2.3 - t_j}\right),$$
$$t_j = (0.001j)s, 1 < j < 2000$$

CWT peaks lose power toward higher frequencies, it is misleading since the amplitudes of the chirp signals are not decreasing over time.

Using the window parameters set, the true signal peaks are very well resolved and their percentage variance does not significantly change across the time-frequency domain.

Weighted LSWS using the Gaussian values as weights tunes the spikes in Fig. 3c (white arrows). The spikes are mitigated, but the bandwidth of the spectra increases (see inside the circles)

Weighted LSWS using power spectral density representation in terms of decibel (dB).

3) Weighted Wavelet Z transform (WWZ) vs least-squares wavelet analysis (LSWA)

Simulation of unequally spaced time series for 1 month, consisting of trend, non-stationary signal, random noise and hyperbolic chirp signal. The known frequencies are suppressed to reveal the hidden signals (see Fig. 5).

WWZ is a poor measure of amplitude; however, the constituents of known forms are explicitly considered in the LSWA (see the difference between the right and left hand sides of Fig. 5.

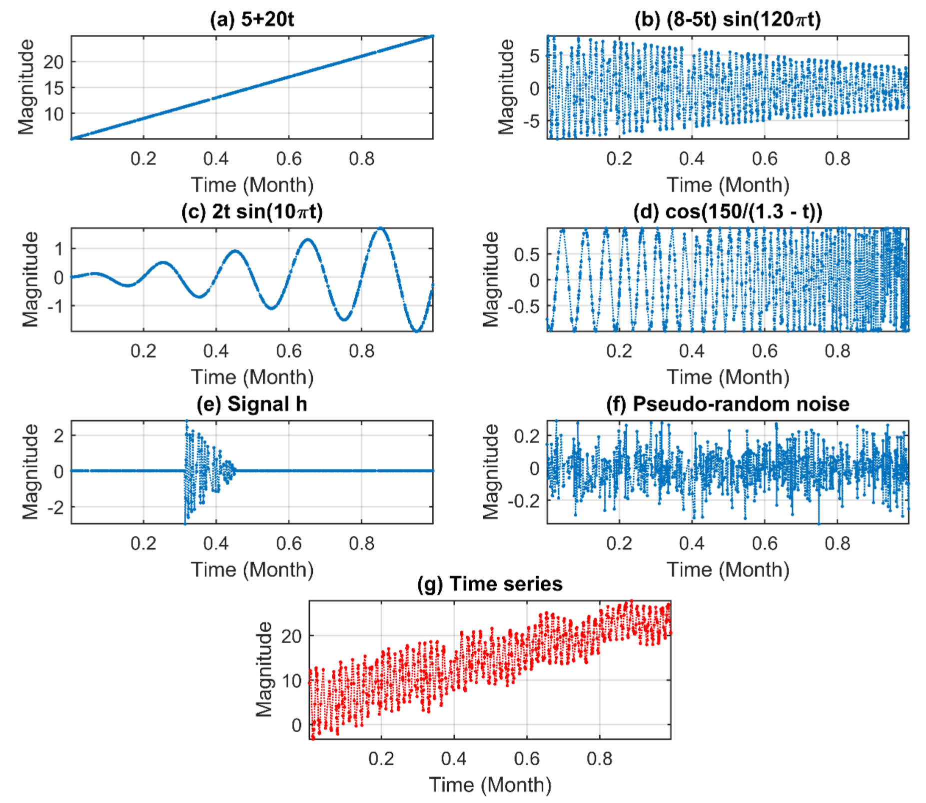

Fig. 4) The unequally spaced time series and its constituents. **(a)-(f)** different constituents and **(g)** the time series (the sum of the constituents).

Note: LSWA clearly shows the hidden signals after simultaneously removing the constituents of known forms (red circles in Fig. 5).

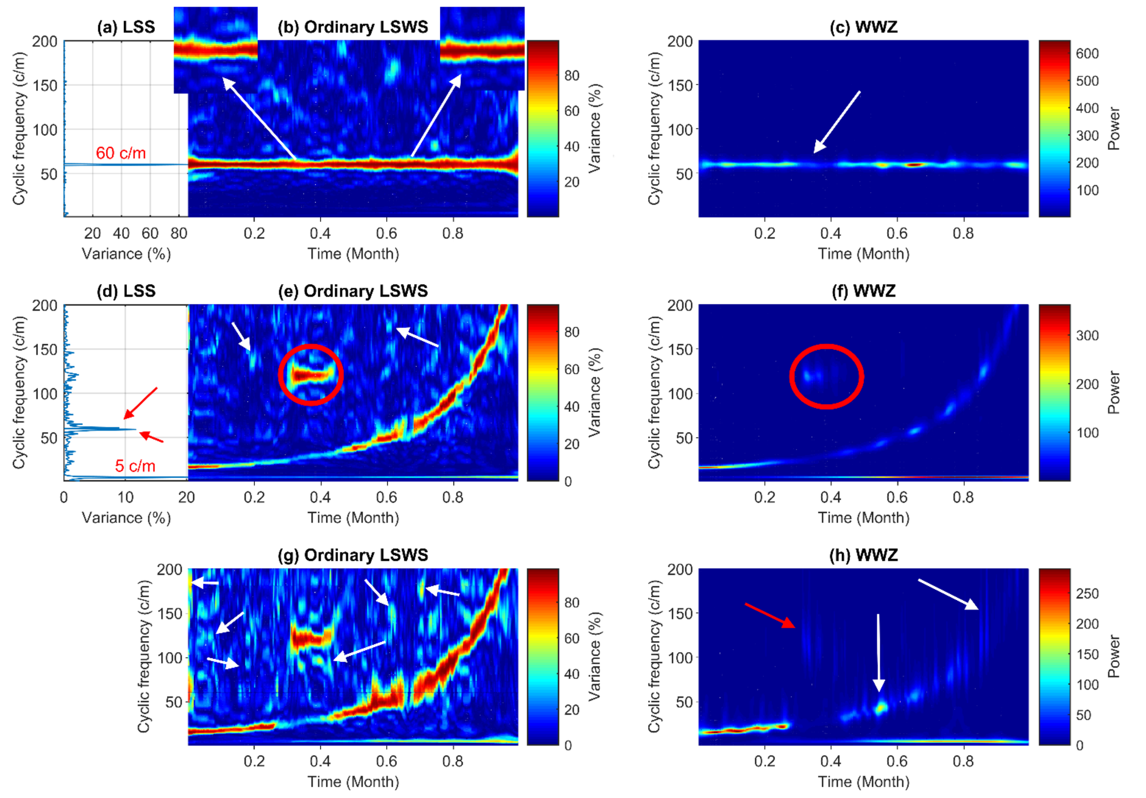

Fig. 5) De-trended time series **(a)** Least-squares spectrum (LSS) **(b)** Least-squares wavelet spectrum (LSWS) **(c)** WWZ (note 60 c/m has variable amplitude); **(d)** LSS (does not show the variation of sine wave of 5 c/m) **(e)** LSWS (after simultaneously removing the trend and sine wave of 60 c/m); **(f)** WWZ (after manually removing the trend and sine wave of 60 c/m). **(g)** LSWS with modified window parameters **(h)** WWZ with modified c=0.1

4)Least-squares cross wavelet spectrogram (LSCWS)

Synthetic time series:

$$f_1(t_i) = \cos\left(\frac{30}{1.2 - t_i}\right) + g(t_i) + w_1, 0 \le t_i \le 1, 1 \le i \le 600,$$
$$g(t_i) = \cos(25(2\pi t_i)), 200 \le i \le 300$$

$$f_2(t_j') = \cos(5(2\pi t_j')) + \cos\left(25(2\pi t_j') + \frac{\pi}{2}\right) + w_2, 0 \le t_j' \le 1, 1 \le j \le 400$$

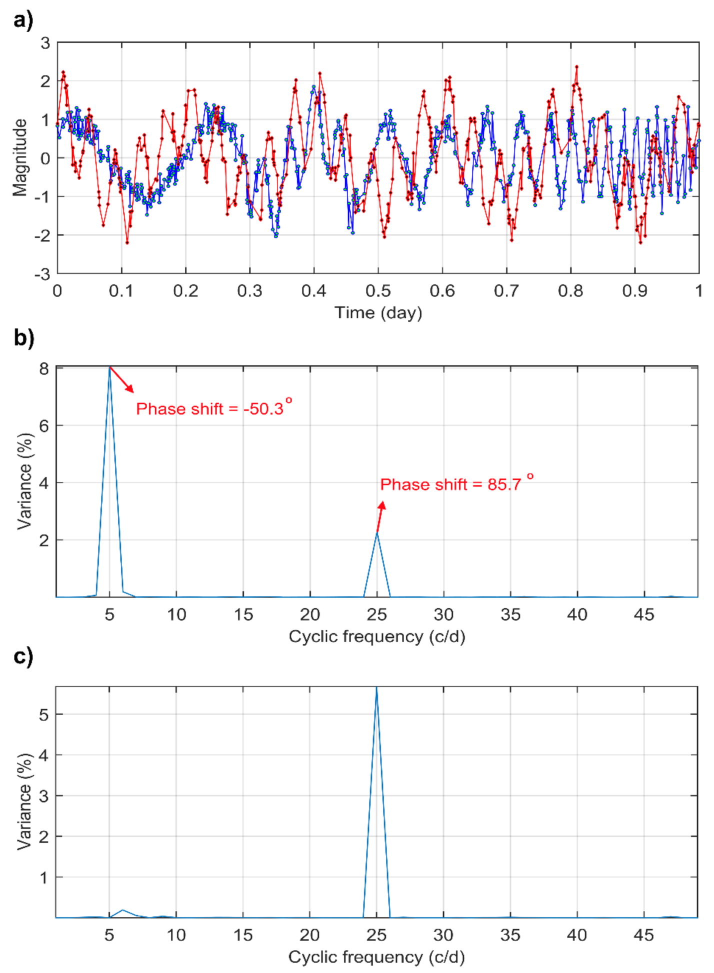

Fig. 6) **(a)** Two unequally spaced series **(b)** Least-squares cross spectrum (LSCS) of the two time series **(c)** LSCS of the two residual time series after suppressing the peak at 5 c/d

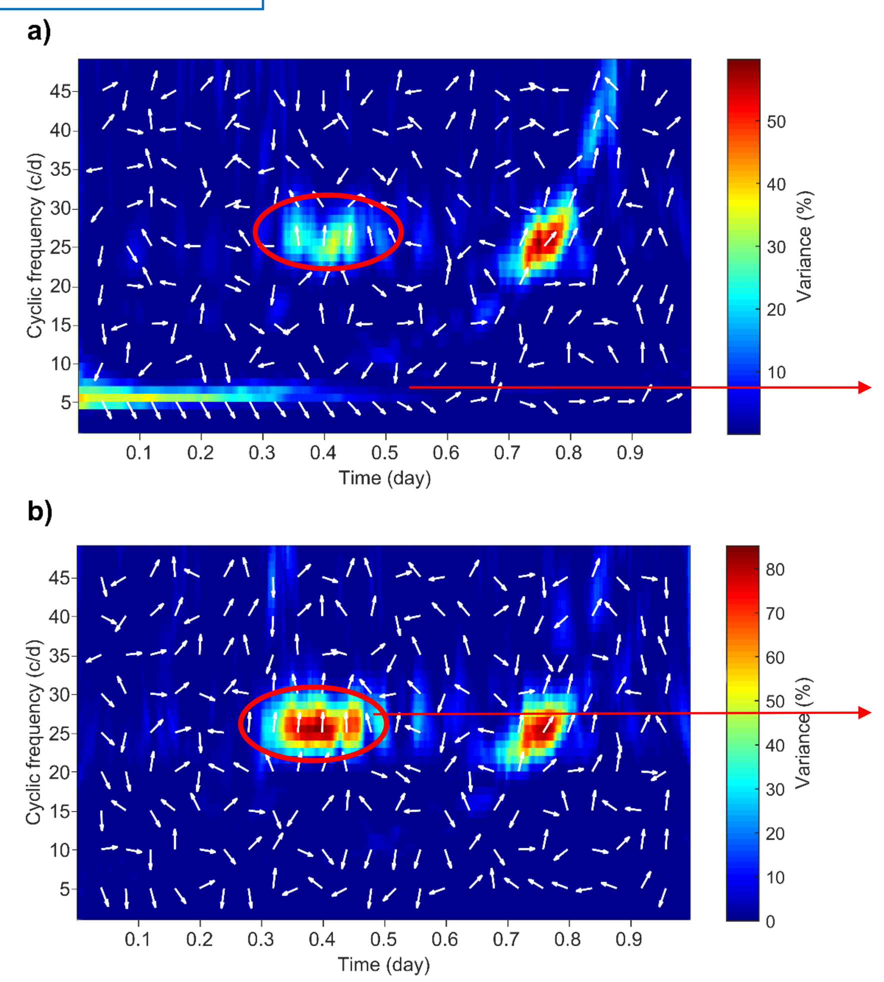

Fig. 7) **(a)** LSCWS of the time series **(b)** LSCWS of the residual time series after removing (suppressing) the peaks at 5c/d. The arrows on the spectrogram show the phase differences.

The % variance of the 5c/day (c/d) corresponding peak decreases as time increases. Since the frequency of the hyperbolic chirp in f_1 increases rapidly over time, it shows less coherency with the cosine wave of 5c/d of f_2.

The coherency increases after the 5c/d is removed and 90 degrees phase difference between the time series is observed.

5) GOCE gradiometer measurements and Poynting energy flux

LSCWA is used effectively to study the disturbances in the gravitational gradients observed by GOCE satellite that arise from plasma flow in the ionosphere. (GGT-Gravitational gradient tensor)

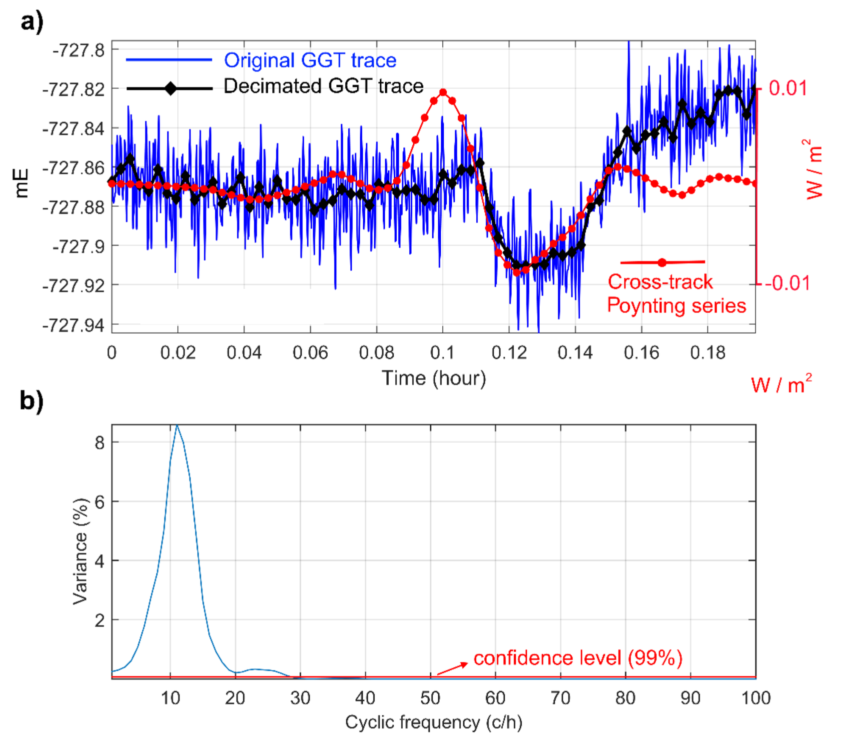

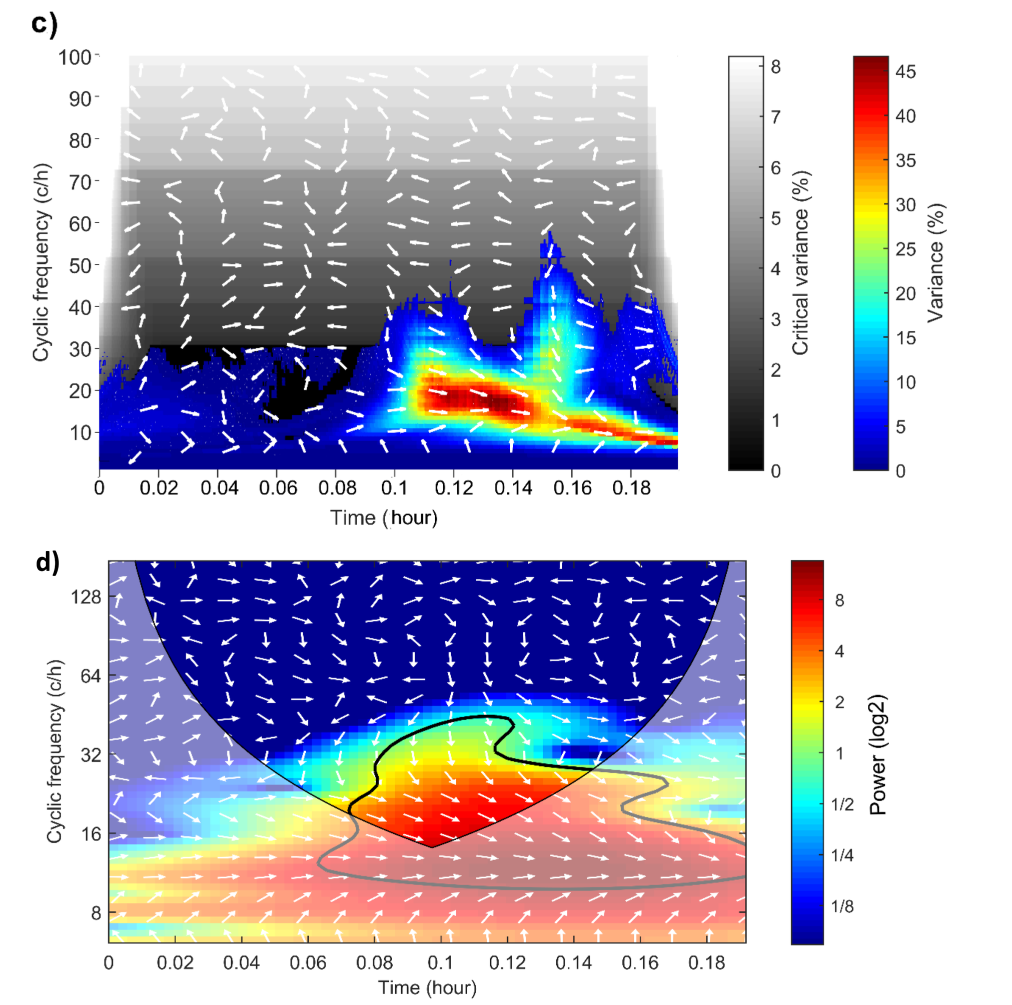

Fig. 8) **(a)** The cross-track Poynting vector component (W/m^2) and decimated GGT trace series (miliEotvos) for a satellite track **(b)** The LSCS of original GGT trace and cross-track Poynting vector component series with 99% confidence level **(c)** LSCWS of the Poynting vector and the original GGT trace series with the stochastic surface at 99% confidence level (gray colour bar) and phase differences (arrows) **(d)** The cross wavelet transform (XWT) of the Poynting vector and the decimated GGT trace series (MATLAB).

Note: LSCWA does not require the two time series to be equally spaced or have the same sampling rate.

6) VLBI (Very Long Baseline Interferometry) baseline length and atmospheric temperatures

LSCWA is also used to study the coherency between the Westford-Wettzell VLBI baseline length and the temperature series at both stations, showing significant thermal effects on the baseline length.

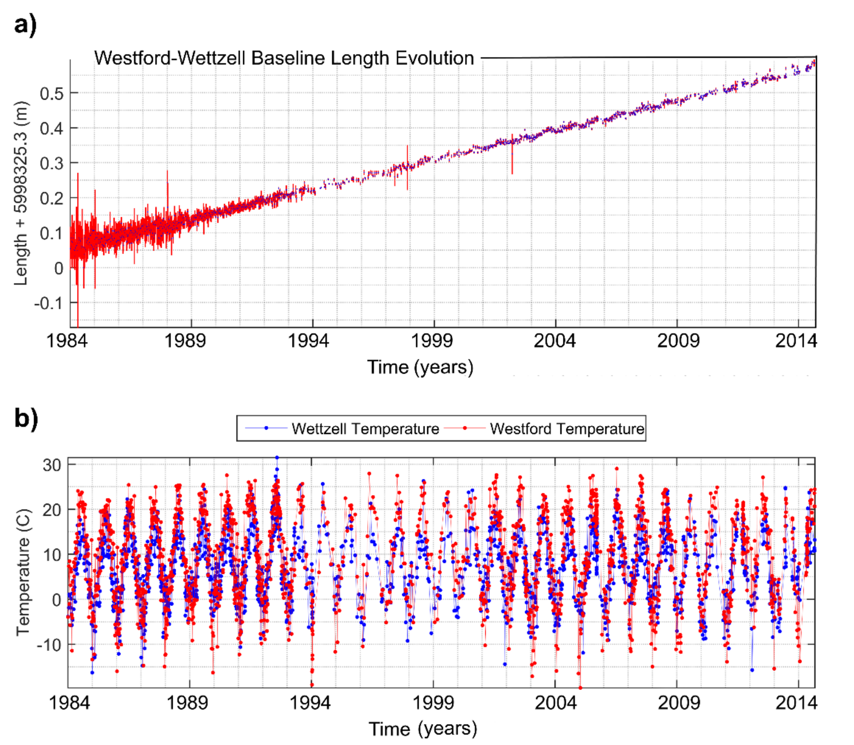

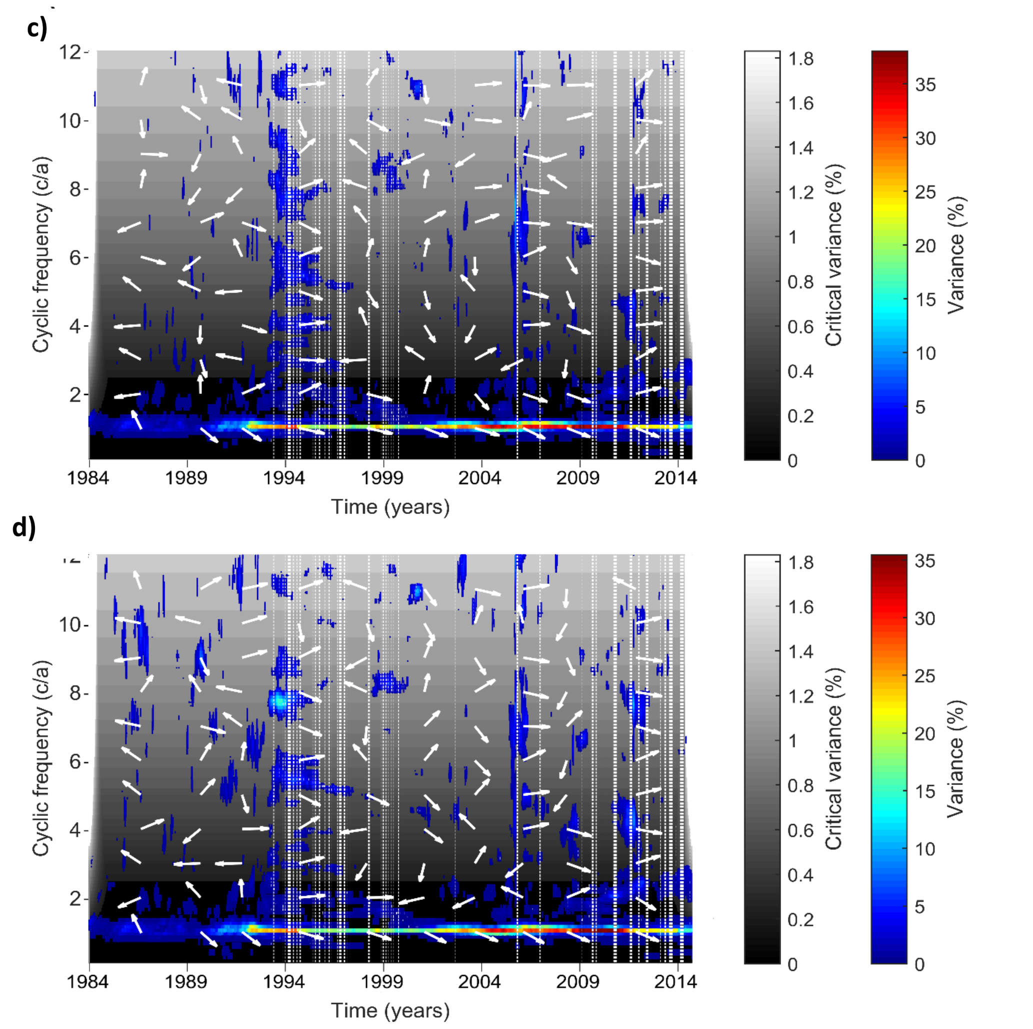

Fig. 9) **(a)** The unequally spaced VLBI baseline length evolution since January 1984 with error bars (red) **(b)** Unequally spaced and equally weighted temperature series at stations Westford (red) and Wettzell (blue) since January 1984. **(c) and (d)** The LSCWS of the residual VLBI series (baseline length and temperature) in Westford and Wettzell, respectively with their stochastic surfaces at 99% confidence level (gray) and phase differences (white arrows).

References

Ghaderpour, E., Ince, E.S., & Pagiatakis, S. D. (2018). Least-squares cross wavelet analysis and its applications in geophysical time series, *Journal of Geodesy*, revised version is submitted.

Ghaderpour, E., & Pagiatakis, S. D. (2017). Least-Squares Wavelet Analysis of Unequally Spaced and Non-stationary Time Series and Its Applications. *Mathematical Geosciences*, *49*(7), 819-844.

Ince, E. S., & Pagiatakis, S. D. (2016). Effects of space weather on GOCE electrostatic gravity gradiometer measurements. *Journal of Geodesy*, *90*(12), 1389-1403.

Pagiatakis, S. D. (1999). Stochastic significance of peaks in the least-squares spectrum. *Journal of Geodesy*, *73*(2), 67-78.